Reduction of Monophosphaallenes: An EPR Study and ab Initio Investigations of $(HPCCH_2)^{-\bullet}$ and $(HPCHCH_2)^{\bullet}$ Radicals

Mostafa Chentit, Helena Sidorenkova, and Michel Geoffroy*

Department of Physical Chemistry, University of Geneva, 30 quai Ernest Ansermet, 1211 Geneva, Switzerland

Yves Ellinger*

Laboratoire d'Etude Théorique des Milieux Extrêmes, Ecole Normale Supérieure, 24 rue Lhomond, 75005, Paris, France

Received: June 8, 1998; In Final Form: October 7, 1998

Cyclic voltammetry shows that monophosphaallene $ArP{=}C{=}C(C_6H_5)_2$ (where Ar = $C_6H_2{}^tBu_3$-2,4,6), **1a,** undergoes irreversible reduction at 2266 mV in THF. The EPR spectra of the reduction products are obtained in liquid and frozen solutions after specific ^{13}C enrichment of the allenic carbon atoms. The resulting hyperfine tensors are compared with those obtained from ab initio MP2, MCSCF, CI, and DFT calculations for the radical anion $(HP{=}C{=}CH_2)^{-\bullet}$ and for the monophosphaallylic radical $(HP^{\bullet}{-}CH{=}CH_2) \leftrightarrow (HP{=}CH{-}{}^{\bullet}CH_2)$. The most elaborate treatments of the hyperfine structure (CI and DFT) indicate that the species observed by EPR is the monophosphaallylic radical.

Introduction

The past decade has been marked by considerable developments in the chemistry of low-coordinated phosphorus compounds.[1] A large variety of new organic molecules containing a trivalent dicoordinated phosphorus atom have been synthesized. Most of these molecules present interesting properties in coordination chemistry,[2] and recent investigations have shown that they are often good electron acceptors.[3,4] In the present paper, our objective is to explore the possibilities of adding an electron to monophosphaallene[5] **1a** and to determine the electronic structure of the corresponding reduction compound.

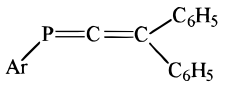

1a

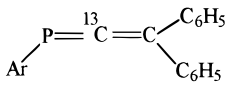

1a$_1$

Ar: $C_6H_2{}^tBu_3$-2,4,6

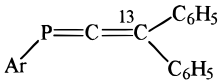

1a$_2$

Two approaches are generally used to obtain structural information about a paramagnetic species: (1) A spectroscopic approach which characterizes the radical by its hyperfine couplings and which interprets these parameters in terms of spin densities. (2) Quantum mechanical investigations which lead to the wave function of the open-shell system in its equilibrium structure.

Several difficulties are expected to appear when applying these methods to the products resulting from the reduction of **1a**. On one hand, since this system is likely to be delocalized on three atoms, a reliable analysis of the experiments requires that the spin densities must be obtained on two carbons which, a priori, do not bear any α-proton; moreover, an eventual π structure implies that the isotropic hyperfine couplings which result from indirect mechanisms (spin polarization) are probably not very suitable for providing information about the spin delocalization. On the other hand, ab initio predictions of the isotropic couplings using a single-determinant representation of the wave function, even amended by Moller−Plesset perturbation theory, are expected to be rather inaccurate for three-electrons, three-centers π systems and spin-clean calculations are necessary.

To facilitate the analysis and the interpretation of our results, the following strategy has been adopted: (i) synthesis of specifically ^{13}C-enriched compounds $ArP{=}{}^{13}C{=}C(C_6H_5)_2$ (**1a$_1$**) and $ArP{=}C{=}{}^{13}C(C_6H_5)_2$ (**1a$_2$**) followed by electrochemical reduction have been carried out. (ii) The EPR spectra have been recorded in both liquid and frozen solutions in such a way as to measure the Fermi-contact interaction as well as the dipolar couplings. (iii) Finally, ab initio and DFT calculations of the isotropic and anisotropic coupling constants have been performed for model compounds where the aryl groups have been replaced by hydrogen atoms. Owing to the well-known but still unpredictable artifacts that may spoil the calculations of EPR parameters according to the method used, particular attention has to be paid to this theoretical part.

Finally, it is shown that when all these conditions are fulfilled, a joint interpretation of the EPR measurements and ab initio calculations leads to an unambiguous identification of the reduction product of **1a**.

Experimental Section

Compounds. Molecule **1a** has been synthesized by reacting, after lithiation with ^{n}BuLi, $ArP{=}CCl_2$[6] with $ClSiMe_3$ and reacting the resulting phosphaalkene $ArP{=}C(C1)SiMe_3$[7] with ^{t}BuLi; finally, benzophenone was added to the reaction mixture. The product **1a** was purified by recrystallization from hexane. These reaction sequences were also followed for the synthesis of **1a$_1$** and **1a$_2$**, using, respectively, $H^{13}CCl_3$ and $O{=}{}^{13}C(C_6H_5)_2$ for the preparation of these two isotopically enriched compounds.

10.1021/jp982519b CCC: $15.00
Published on Web 12/01/1998

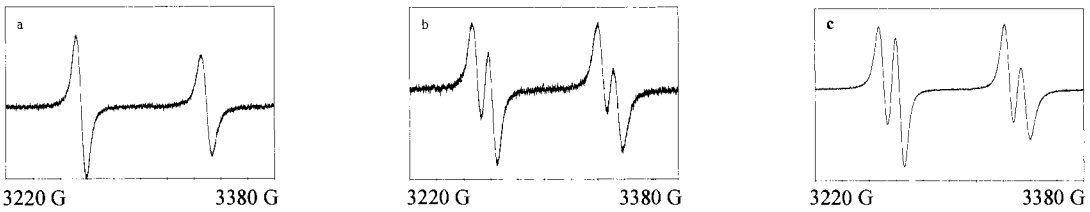

Figure 1. EPR spectra obtained at 285 K with an electrochemically reduced solution of (a) ArP═C═C(C_6H_5)$_2$, (b) ArP═^{13}C═C(C_6H_5)$_2$, (c) ArP═C═^{13}C(C_6H_5)$_2$.

Instrumentation. Cyclic voltammetry measurements were carried out on a BAS station (model CV-50W) with a platinum electrode, an SCE reference electrode, and tetrabutylammonium hexafluorophosphate (10^{-1} M) as the electrolyte. EPR spectra were recorded on a Bruker 200D spectrometer (X-band, 100 kHz field modulation) equipped with a variable-temperature attachment. NMR spectra of all compounds were obtained prior to EPR studies. The analysis of all EPR spectra was controlled by numerical simulation.[8]

Computations. The ab initio calculations were performed with GAUSSIAN94 [9] for UHF, MP2, and density functional levels of theory. MCSCF calculations used HONDO8.5,[10] and CI treatments were carried out with the MELDF[11] package.

Results and Discussion

EPR Spectra. Cyclic voltammetry of **1a** shows that this compound undergoes irreversible reduction at −2266 mV in THF and at −1965 mV in DMF. The in situ electrolysis, inside the EPR cavity, of a solution of **1a** in THF leads, at 285 K, to an EPR spectrum characterized by a ^{31}P isotropic coupling constant of 262 MHz (Figure 1a). As shown in Figure 1b, when this experiment is carried out with the ^{13}C-enriched compound **1a$_1$**, an additional splitting of 33 MHz is observed, whereas isotopic enrichment of the terminal carbon (**1a$_2$**) gives rise to an additional coupling of 34 MHz (Figure 1c).

The EPR spectra are drastically modified when the temperature of the electrolyzed solution is lowered from 285 to 150 K. A broadening of the signals occurs between 285 and 160 K, which principally affects the external lines. Below 150 K, any motion of the paramagnetic species is frozen and the resulting "powder-type" spectra are characterized by an axial ^{31}P hyperfine tensor. The trace of this tensor is totally consistent with the value of A_{iso} measured in the liquid phase. The ^{13}C coupling is easily measured on the external lines ("parallel" components of the phosphorus hyperfine structure). For **1a$_1$**, this splitting is equal to 45 MHz; this value together with the isotropic constant of 33 MHz imply, in the hypothesis of an axial ^{13}C coupling tensor, a "perpendicular" coupling of 27 MHz. Similarly, the ^{13}C splitting of 79 MHz observed on the external lines of **1a$_2$** together with the isotropic coupling of 34 MHz imply a "perpendicular" coupling of 11.5 MHz for the terminal ^{13}C.

It is worth mentioning that the simulation of the frozen solution spectra[8] with the above parameters, on the hypothesis of aligned axial g,^{31}P, and ^{13}C coupling tensors, leads to a fitting which is not perfect for the central parts of the spectra of **1a$_1$**: when the line width is adjusted to fit the external lines, the simulation predicts that, in contrast to the experimental spectrum, some ^{13}C splitting would be detected in the central pattern. This implies that an additional small interaction is probably present which affects the perpendicular region more than the parallel one. As shown in Figure 2, satisfactory simulations were obtained by using the tensors given in Table 1 together with an additional proton coupling tensor: $T_x = 8$ MHz, $T_y = 20$ MHz, $T_z = 4$ MHz (with the z axis aligned along the ^{31}P−$T_{||}$ direction).

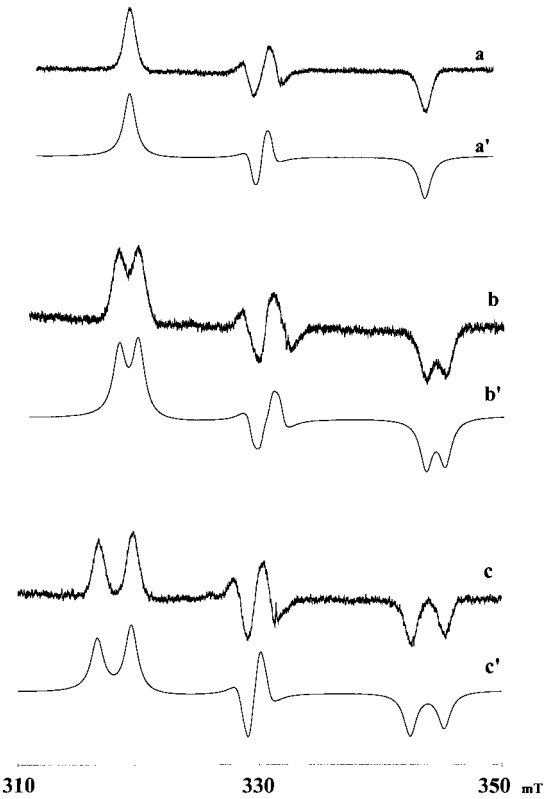

Figure 2. EPR spectra obtained at 110 K with an electrochemically reduced solution of (a) ArP═C═C(C_6H_5)$_2$, (b) ArP═^{13}C═C(C_6H_5)$_2$, (c) ArP═C═^{13}C(C_6H_5)$_2$. a′, b′, and c′ are the corresponding simulated spectra (see text).

The decomposition of the ^{31}P and ^{13}C hyperfine tensors into isotropic and anisotropic coupling constants (Table 1) clearly shows that, in the reduced species, the unpaired electron is mainly localized on the phosphorus atom. Comparison of the experimental isotropic and anisotropic interactions with the corresponding atomic coupling constants[12] (^{31}P, $A^*_{iso} = 13\,306$ MHz, $2B_o = 733$ MHz; ^{13}C, $A^*_{iso} = 3777$ MHz, $2B_o = 214$ MHz) leads to the spin densities given in Table 2.

The very small s character of the magnetic orbital together with the large participation of phosphorus and terminal carbon p atomic orbitals are indicative of a π type SOMO, the isotropic coupling constants being mainly due to spin polarization. As shown in Table 3, these features are not in conflict with the properties expected for a $(RP{=}C{=}CR'_2)^{-\bullet}$ radical anion.

Quantum Mechanical Calculations. Phosphaallenic derivatives, such as **1a**, in which three aromatic groups are attached to the allenic P═C═C linkage are still far beyond the attainable targets for today's quantitative ab initio methods. Simpler model systems have to be considered. For phosphorus species containing allenic systems, we have shown that replacement of the cumbersome aryl groups by hydrogens provides model com-

TABLE 1: EPR Parameters from the Observed Spectra

species	tensor	eigenvalues[a]	isotropic coupling[a] liquid	isotropic coupling[a] frozen	anisotropic coupling[b]
1a	g	$g_{//}$ 2.0027, $g_{\perp}$ 2.0094			
	^{31}P (MHz)	$T_{//}$ 725, $T_{\perp}$ 30	262	262	$\tau_{//}$ 463, $\tau_{\perp}$ − 232
1a$_1$					
	^{31}P (MHz)	$T_{//}$ 725, $T_{\perp}$ 30	262	262	$\tau_{//}$ 463, $\tau_{\perp}$ − 232
	$^{13}C_{(1)}$ (MHz)	$T_{//}$ 45, $T_{\perp}$ 23	33	30	$\tau_{//}$ 15, $\tau_{\perp}$ −7.5
1a$_2$					
	^{31}P (MHz)	$T_{//}$ 725, $T_{\perp}$ 30	262	262	$\tau_{//}$ 463, $\tau_{\perp}$ −232
	$^{13}C_{(2)}$ (MHz)	$T_{//}$ 79, $T_{\perp}$ 12.5	34	35	$\tau_{//}$ 44, $\tau_{\perp}$ − 22

[a] Only the absolute values of the coupling constants are known. The $T_{\perp}$ values are obtained from a simulation of the frozen solution spectra (see text). [b] Only the relative signs of the anisotropic coupling constants are known.

TABLE 2: Experimental Spin Densities

atom	s spin density	p spin density
phosphorus	0.019	0.616
C_1 (central carbon)	0.008	0.059
C_2 (terminal carbon)	0.009	0.202

TABLE 3: Hyperfine Interaction for Diphosphaallene and Monophosphaalkene Radical Anion

radical anion	^{31}P coupling (MHz)	^{13}C coupling (MHz)
$(ArP{=}{}^{13}C{=}PAr)^{-\bullet}$ [4]	$A_{iso} = 215$	$A_{iso} = 27$
$(ArP{=}{}^{13}C(H)C_6H_5)^{-\bullet}$ [5]	$A_{iso} = 152$	$A_{iso} = 16$
	$\tau_{//} = 303$	$\tau_{//} = 31$

pounds which retain the main characteristics of the larger systems for neutral molecules as well as for the positive[13] and negative ions.[4] Applying the same philosophy to the present class of allenic species points to **2** as the proper model system.

1. The Diamagnetic Molecule 2. Before we verify to what extent the above interpretation is consistent with the EPR experiments we first consider the parent molecule **2**. The

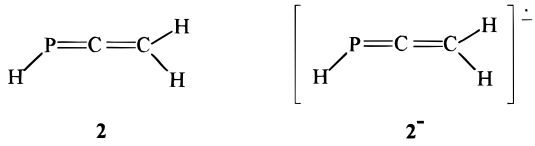

2 **2$^-$**

optimized geometry obtained at several levels of theory (MP2/6-311G**, MCSCF/6-311G**, and B3LYP/6-311G**) is reported in Table 4.

The results of the RHF/3-21G* calculations are presented only to show the level of quality which can be expected for large systems when using this cost-effective atomic representation. Anticipating the breakdown of the allenic system with reduction, we also performed MCSCF/6-311G** calculations whose active space includes all valence orbitals. In terms of a localized orbital description of the σ backbone, the electronic configurations are generated by distributing the 16 valence electrons into 15 orbitals:

$$[\text{core}]^{14}\,[\sigma_{PH}\,\sigma_{CH}\,\sigma_{CH}\,\sigma_{PC}\,\sigma_{CC}\,1p_P\,\pi\,\pi\,\pi^*\,\pi^* \times \sigma_{PH}^*\sigma_{CH}^*\,\sigma_{CH}^*\,\sigma_{PC}^*\,\sigma_{CC}^*]^{16}$$

In this treatment, the core consists of the inner shells of the two carbons and phosphorus atoms. All antibonding orbitals are used in the definition of the active space, and internal excitations are limited to singles and doubles with respect to the reference determinant. This level ensures a correct treatment of electronic correlation for structural studies.[14]

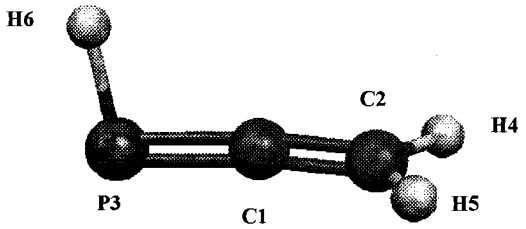

Figure 3. Optimized structure for monophosphaallene HP=C=CH$_2$.

The C_s geometry found for HP=C=CH$_2$ is typical of allenic compounds with the PH bond in a plane perpendicular to the HCH plane (Figure 3).

The difference from allene is that the replacement of one of the CH$_2$ groups by PH induces a slight distortion of the P=C=C skeleton from linearity (∼5°). This distortion is inferior to that observed for P=C=P in diphosphaallene[13] at the same level of theory (∼10°). The C=C bond is close to that of allene, and P=C is the same as in HP=C=PH. Comparison of the calculated geometry with the structural parameters deduced from X-ray diffraction on the bulky compound **1a**[5] shows the validity of the model. The main difference is the opening of the RPC angle with respect to HPC as a consequence of steric repulsion. It should also be mentioned that these results obtained with extended basis sets and correlated wave functions do not change the previous results[15] significantly.

2. The Negative Ion **2$^-$.** The same series of calculations was performed on the negative ion, including correlation effects at

TABLE 4: Optimized Parameters[a] and Energies (au) for HP=C=CH$_2$

	RHF/3-21G*	MP2/6-311G**	MC/6-311G**	B3LYP/6-311G**	exp[b]
E	−416.07288	−418.71830	−418.33372	-419.34557	
C(1)−C(2)	1.292	1.316	1.319	1.304	1.310
P(3)−C(1)	1.624	1.646	1.655	1.646	1.628
C(2)−H(4)	1.075	1.087	1.095	1.087	
P(3)−H(6)	1.409	1.417	1.435	1.432	
P(3)C(1)C(2)	176.47	173.36	174.96	173.84	167.7
H(4)C(2)C(1)	121.44	121.01	121.18	121.42	122.4
H(4)C(2)H(5)	117.12	118.98	117.64	117.14	117.2
H(6)P(3)C(1)	97.05	94.92	96.93	95.95	103.9
H(6)P(3)C(2)H(4)	91.12	91.52	91.19	91.60	−91.5

[a] Bond lengths in Angströms; bond and torsion angles in degrees. [b] The experimental data are obtained from the crystal structure of **1a**.

TABLE 5: Optimized Parameters[a] and Energies (au) for the Radical Anion $(HP{=}C{=}CH_2)^-$

	cis-like				trans-like			
	UHF-3-21+G*	MP2-6-311++G**	MC-6-311++G**	B3LYP-6-311++G**	UHF-3-21+G*	MP2-6-311++G**	MC-6-311++G**	B3LYP-6-311++G**
E	−416.07139	−418.70022	−418.28706	−419.35056	−416.07367	−418.70503	−418.29000	−419.35369
Δ*E* (kcal)	1.4	3.0	1.8	2.0	0.0	0.0	0.0	0.0
C(1)−C(2)	1.334	1.323	1.343	1.331	1.332	1.324	1.345	1.335
C(1)−P(3)	1.761	1.688	1.769	1.726	1.767	1.706	1.769	1.740
H(4)−C(2)	1.084	1.100	1.110	1.103	1.085	1.100	1.110	1.102
H(5)−C(2)	1.081	1.091	1.105	1.093	1.081	1.092	1.103	1.093
H(6)−P(3)	1.429	1.442	1.456	1.456	1.417	1.421	1.422	1.438
P(3)C(1)C(2)	155.78	150.44	149.05	149.88	144.85	138.57	140.65	140.31
H(4)C(2)C(1)	122.08	122.02	122.56	122.70	122.37	122.75	123.22	123.09
H(5)C(2)C(1)	122.11	122.82	122.61	122.85	122.00	155.18	122.02	122.32
H(4)C(2)H(5)	115.81	115.15	114.83	114.46	115.63	115.03	114.74	114.58
H(6)P(3)C(1)	96.99	99.94	98.48	98.96	96.38	98.14	97.75	97.80
H(4)C(2)C(1)P(3)	2.18	17.83	9.31	8.63	10.47	23.92	16.07	18.32
H(6)P(3)C(2)H(4)	20.19	50.25	46.92	53.64	127.32	122.24	119.76	121.64

[a] Bond lengths in Angströms; bond and torsion angles in degrees.

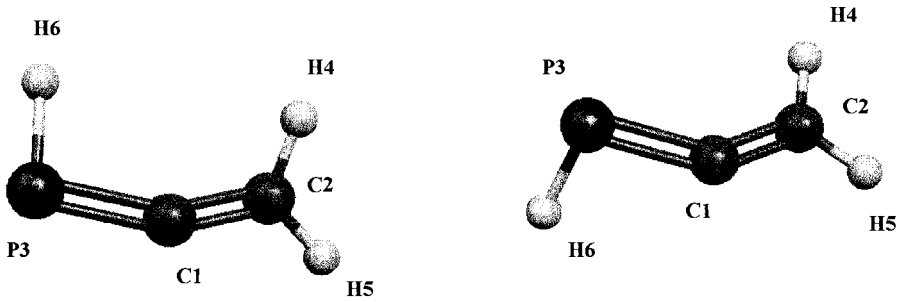

Figure 4. Optimized structures for the two isomers of the monophosphaallenic radical anion $(HP{=}C{=}CH_2)^-$.

TABLE 6: Infrared Frequencies (cm^{-1}) and Intensities (km/mol) for $HP{=}C{=}CH_2$[a] and Its Negative Ions[b]

		$H-P{=}C{=}CH_2$		$H-P{=}C{=}CH_2^-$ cis-like		$H-P{=}C{=}CH_2^-$ trans-like	
assignment	irep	*ν*	*I*	*ν*	*I*	*ν*	*I*
PCC bend	A′	305	8	191	6	247	13
PCC bend	A″	315	12	275	12	312	14
$HPCCH_2$ tors	A″	736	0	498	35	534	35
PC stretch	A′	759	0	605	33	630	28
CH_2 wag	A′	859	53	712	44	728	43
HPC bend	A′	888	33	764	53	815	23
CH_2 rock	A″	943	2	920	25	931	25
HCH bend	A′	1367	0	1299	50	1295	60
CC stretch	A′	1764	74	1461	108	1454	91
PH stretch	A′	2259	88	1942	326	2063	242
CH_2 stretch (sym)	A′	3028	0	2672	289	2689	248
CH_2 stretch (asym)	A″	3097	0	2784	84	2789	84

[a] B3LYP/6-311G**. [b] B3LYP/6-311++G**

the MP2/6-311++G** and MCSCF/6-311++G** levels of theory. The structural parameters are reported in Table 5.

The UHF/3-21+G* results are also presented in view of possible application to larger systems. The MCSCF treatment is adapted from the neutral system by adding one more electron to the valence space. Diffuse functions have been systematically added to the basis set to account for the spatial extension of the wave function.

As for diphosphaallene radical anion $HP{=}C{=}PH^-$, two minimum energy structures, cis-like and trans-like (Figure 4), are found which differ from the neutral allenic parent by opposite rotation of the P−H bond. The trans-like minimum is more stable by about 1.8−3.0 kcal/mol. The two structures also differ in the value of the PCC bending angles. The trans-like minimum has a PCC angle of ∼140°, whereas it opens by 10° in the cis-like minimum due to the repulsion between the PH and CH bonds. In accord with the lower strength of the phosphorus−carbon π bond compared to the carbon−carbon π bond, the formation of the anion leads to a larger increase of the P=C bond than of the C=C bond.

These two geometries are true minima as proved by the vibrational analysis reported here at the B3LYP/6-311++G** level together with that of the neutral parent (Table 6).

Frequencies have been scaled by 0.975 according to the prescription by Bauschlicher and Langhoff.[16] There are two important consequences following the addition of one electron in the π orbitals: first, a general shift of all vibrations to lower frequencies, which shows the weakness introduced in the allenic system, and second, a strong increase in the band strengths since the total integrated intensity in the ion is 1065 (cis-like) or 906 km/mol (trans-like) compared to 270 km/mol in the neutral. The breaking of the conjugated system also changes the coupling between vibrations. The PC stretching which was strongly mixed with the CC stretching in the neutral molecule is well-separated in the ion, the CC stretching at 1441−1434 cm^{-1} now being

TABLE 7: Calculated Isotropic and Anisotropic Coupling Constants (MHz) for $(HP{=}C{=}CH_2)^-$

	cis-like					trans-like				
	UHF-3-21+G*	MP2-6311++G**	B3LYP-6311++G**	SCI-631+G*	SCI-aug-cc-pVDZ	UHF-3-21+G*	MP2-6311++G**	B3LYP-6311++G**	SCI-631+G*	SCI-aug-cc-pVDZ
A_{iso} ^{13}C(1)	165	−118	119	190	184	183	−104	139	133	133
A_{iso} ^{13}C(2)	−34	217	22	2	−8	−22	228	28	44	45
A_{iso} ^{31}P(3)	125	344	291	113	180	−14	118	−12	73	70
τ ^{13}C(1)	113	122	91	110	112	96	120	90	88	90
	−47	4	−44	−58	−52	−58	−129	−48	−45	−46
	−66	−126	−47	−52	−60	−38	9	−42	−43	−44
τ ^{13}C(2)	−15	−54	−2	−2	−3	−15	−55	−5	−5	−5
	2	−53	−6	−7	−6	2	−55	−3	−2	−2
	13	107	8	9	9	13	110	8	7	7
τ ^{31}P(3)	−11	−57	−78	−62	−40	84	200	191	171	167
	20	90	149	122	83	−38	−76	−92	−81	−80
	−9	−33	−71	−60	−43	−46	−124	−99	−90	−87

coupled with the nearby HCC bending at 1281−1277 cm^{-1}. The EPR parameters calculated for the two minima are reported in Table 7. In view of the large spin contamination of the UHF wave function, CI calculations in a basis of spin-adapted configurations were performed to ensure a spin-clean treatment of the spin-dependent observable, i.e., a CI wave function that is an eigenfunction of S_z as well as S.[2] In this latter case, the MCSCF/6-311++G** optimized geometry were used.

Two basis sets were employed: 6-31+G* and aug-cc-pVDZ.[17] The first one is a smaller but well-balanced basis set which is well-suited to the CI treatment of negative ions;[18] the second one was selected after systematic investigations of phosphorus-containing simple radicals. It was verified that the choice of the method used for the geometry optimization does not change the results by more than a few percent.

From the values of Table 7 (and other calculations not reported here), it is clear that none of the wave functions can reproduce the experimental spectra. This is true not only for UHF, UMP2, and DFT treatments but also for the spin-adapted CI calculations.

This result is not too surprising for isotropic coupling constants. It is well-known, indeed, that the values of A_{iso} are difficult to obtain with accuracy since they depend on the local value of the spin density at the nuclei. UHF and MP2 calculations are irrelevant in this study because of spin contamination. However, SCI calculations which contain all single excitations from the reference determinant in order to account for the dominant spin-polarization effects generally provide better than qualitatively correct A_{iso} values. Here, they are often off by 1 order of magnitude (experimental values (MHz) $A_{iso}(^{13}C(1)) = 33$; $A_{iso}(^{13}C(2)) = 34$; $A_{iso}(^{31}P) = 262$; cis-like SCI(MHz) $A_{iso}(^{13}C(1)) = 190$; $A_{iso}(^{13}C(2)) = 2$; $A_{iso}(^{31}P) = 113$; trans-like SCI(MHz) $A_{iso}(^{13}C(1)) = 133$, $A_{iso}(^{13}C(2)) = 44$; $A_{iso}(^{31}P) = 73$). DFT values do not show any better agreement.

Turning to anisotropic coupling constants does not show any improvement either. These observables which are linked to the spatial spin distribution are generally handled better at lower levels of wave functions. UHF single-determinant calculations, even with a small spin contamination, are known to provide a good first approximation when a single determinant representation is sufficient (which is not true of the present system). Obviously, the calculated tensors are not related to the measured spectra. Since neither isotropic nor anisotropic couplings could be even approached here, it was clear that the recorded spectra were not the signature of the postulated negative ion.

3. The Neutral Allylic Radical **3**. As mentioned in a preceding section, the simulation of the spectra suggested an additional but small hyperfine interaction that would explain the line width of the frozen solution spectra. The most likely possibility that would provide such an additional coupling is that a hydrogen atom could be attached to the central carbon of the allenic structure. The new model compound **3** can exist, *a priori*, under the two mesomeric forms of an allylic system and is likely to exhibit a preferential localization of the unpaired electron at the phosphorus atom.

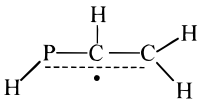

3

Geometry optimizations have been carried out at the same levels of theory as for the negative ion. The MCSCF valence space

$$[\text{core}]^{14}\,[\sigma_{PH}\,\sigma_{CH}\,\sigma_{CH}\,\sigma_{CH}\,\sigma_{PC}\,\sigma_{CC}\,1p_P\,\pi\,\pi\,\pi^* \times \sigma_{PH}^*\sigma_{CH}^*\,\sigma_{CH}^*\,\sigma_{CH}^*\,\sigma_{PC}^*\,\sigma_{CC}^*]^{17}$$

where there are one more σ_{CH} and σ_{CH}^* pair of orbitals but only three π orbitals still contains 17 electrons.

Two minimum-energy structures are also found here, trans and cis, both planar and corresponding to $^2A''$ radicals (Figure 5), but contrary to the previous ions, they are of equal energy. The geometrical parameters are reported in Table 8, and the vibrational analysis is given in Table 9 for both structures.

The two radicals are of allylic type with three electrons in the π system, the unpaired spin being mainly localized on phosphorus as expected. The P=C=C backbone makes an angle of 120−130° characteristic of allylic radicals instead of 140−150° in the ions. The 10° difference between the cis and trans neutral radicals accommodates the repulsion between the PH bond and one of the CH bonds of the methylenic group. The bond lengths are larger in the neutral compounds since addition of a hydrogen atom to the central carbon has broken the in-plane conjugation still partially effective in the phosphaallenic systems. The IR frequencies reflect the structural modifications. The PCC bending shifts to higher wavenumbers in the neutral systems. The opposite shifts of CC (−100 cm^{-1}) and PC (+50 cm^{-1}) with respect to the negative ion is also an illustration of the more balanced electronic distribution in the neutral radical.

The EPR parameters calculated for the two minima are reported in Table 10. As for the negative ion, CI calculations were performed to ensure a spin-clean treatment of the spin-dependent observables using the MCSCF/6-311++G** optimized geometry and the 6-31+G* and aug-cc-pVDZ basis sets.

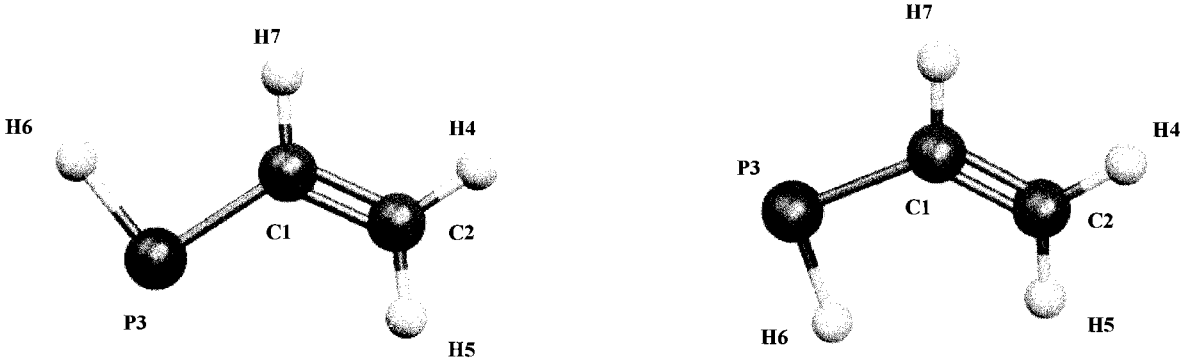

Figure 5. Optimized structures for the two isomers of the monophosphaallylic radical $(HP-CH=CH_2)^{\bullet}$.

TABLE 8: Optimized Parameters[a] and Energies (au) for the Allylic Radical $(HP-CH=CH_2)^{\bullet}$

	cis-like				trans-like			
	UHF-3-21+G*	MP2-6-311++G**	MC-6-311++G**	B3LYP-6-311++G**	UHF-3-21+G*	MP2-6-311++G**	MC-6-311++G**	B3LYP-6-311++G**
E	−416.69654	−419.31854	−418.93014	−419.96154	−416.69658	−419.31845	−418.93022	−419.96158
Δ*E* (kcal)	0.03	−0.06	0.05	0.03	0.00	0.00	0.00	0.00
C(1)C(2)	1.367	1.332	1.357	1.354	1.367	1.332	1.357	1.355
C(1)P(3)	1.772	1.790	1.820	1.785	1.769	1.787	1.815	1.781
H(4)C(2)	1.074	1.085	1.095	1.085	1.075	1.086	1.095	1.085
H(5)C(2)	1.076	1.087	1.096	1.086	1.075	1.086	1.095	1.085
H(6)P(3)	1.405	1.413	1.430	1.427	1.407	1.415	1.433	1.430
H(7)C(1)	1.077	1.087	1.097	1.087	1.079	1.089	1.098	1.089
P(3)C(1)C(2)	122.48	121.32	121.96	122.20	127.34	126.63	127.00	127.73
H(4)C(2)C(1)	121.43	121.79	121.56	121.61	121.25	121.55	121.40	121.44
H(5)C(2)C(1)	121.66	121.49	121.59	121.60	121.76	121.59	121.97	121.68
H(6)P(3)C(1)	97.10	95.89	96.69	96.14	97.09	94.75	96.39	95.80
H(7)C(1)P(3)	119.48	119.93	119.37	119.39	115.11	115.29	114.88	114.43

[a] Bond lengths in Angstroms. [b] Bond and torsion angles in degrees.

TABLE 9: Infrared Frequencies (cm^{-1}) and Intensities (km/mol) for $HP=CH=CH_2$[a]

		$H-P=CH=CH_2$ cis-like		$H-P=CH=CH_2$ trans-like	
assignment	irep	ν	I	ν	I
PH rot	A″	297	45	360	0
PCC bend	A′	328	0	353	2
C−PH wag	A″	510	11	516	7
PC stretch	A′	682	6	666	6
HPC bend	A′	876	16	868	17
CH_2 wag	A″	912	38	907	38
CH wag	A″	968	30	979	24
CH_2 rock	A′	1025	9	1037	15
HCC bend	A′	1264	1	1264	0
CC stretch	A′	1347	11	1360	14
HCH bend	A′	1512	2	1506	1
PH stretch	A′	2295	96	2279	93
CH_2 stretch (sym)	A′	3044	7	3041	8
CH stretch	A′	3062	5	3048	7
CH_2 stretch (asym)	A′	3131	7	3130	10

[a] B3LYP/6-311++G**.

A cursory examination of the calculated hyperfine constants (Table 10) shows that the two isomers have practically the same couplings. The average values obtained from SCI (aug basis set) calculations are in good accordance with the experimental couplings: (1) the three dipolar tensors exhibit axial symmetry and their eigenvalues are similar to the measured values $^{13}C(2)$, $\tau_{\|calc} = 44.5$ MHz, $\tau_{\|exp} = 43$ MHz; ^{31}P, $\tau_{\|calc} = 464.5$ MHz, $\tau_{\|exp} = 465$ MHz;$^{13}C(1)$ $\tau_{\|calc} = -14$ MHz, $\tau_{\|.exp} = -15$ MHz in the hypothesis of three negative eigenvalues for T_{exp} ($^{13}C(1)$). It can also be seen that the B3LYP method provides dipolar tensors which are close enough to experiment to justify its use as a substitute to the SCI treatments. (2) The calculated Fermi contact interactions agree reasonably with the experimental results: $^{13}C(2)$, $A_{iso,calc} = 24.5$ MHz, $A_{iso,exp} = 34$ MHz; ^{31}P $A_{iso,calc} = 216$ MHz, $A_{iso,exp} = 262$ MHz; $^{13}C(1)$ $A_{iso,calc} = -30$ MHz, $A_{iso,exp} = -32.7$ MHz. The calculated isotropic values are satisfactory at the CI-level only, which was to be expected in view of the strong spin contamination of allylic systems. DFT couplings, though more remote from experiments, are still qualitatively correct.

As expected for a π radical, the $\tau_{\|}$ eigenvectors of the ^{31}P, $^{13}C(1)$, and $^{13}C(2)$ couplings are oriented perpendicular to the molecular plane. Due to the specificity of the allylic structure, the calculated values of the Fermi contact (A_{iso}) and of the dipolar interaction ($\tau_{\|}$) for the central carbon are negative. Moreover, the calculated A_{iso} for H(7), attached to the central atom, is positive while the anisotropic coupling of this proton, along the ^{31}P $-$ $\tau_{\|}$, is negative (ca. $-$ 4 MHz). It leads to a total ^{1}H coupling which is small in this direction, whereas the maximum interaction lies in the molecular plane for this proton.

TABLE 10. Calculated Isotropic (A_{Iso}) and Anisotropic (τ) Hyperfine Coupling Constants (MHz) for the Monophosphaallylic Radical ($HP-CH=CH_2$)•

	cis-like					trans-like				
	UHF-3-21+G*	MP2-6311++G**	B3LYP-6311++G**	SCI-631+G*	SCI-aug-cc-pVDZ	UHF-3-21+G*	MP2-6311++G**	B3LYP-6311++G**	SCI-631+G*	SCI-aug-cc-pVDZ
A_{iso} (^{13}C(1))	−49	89	−32	−30	−30	−48	89	−32	−30	−30
A_{iso} (^{13}C(2))	54	−89	27	33	24	54	−89	28	34	25
A_{iso}(^{31}P)	93	−59	109	196	221	93	−62	106	192	212
A_{iso} (^{1}H(7))	20	−53	9	4	4	19	−51	8	4	3
τ (^{13}C(1))	7	35	9	6	6	7	−15	8	6	6
	11	−15	12	8	8	11	34	13	9	9
	−18	−20	−21	−14	−14	−18	−19	−21	−14	−14
τ (^{13}C(2))	−25	−3	−29	−21	−21	−25	0	−29	−21	−22
	−27	0	−30	−22	−23	−27	−3	−31	−23	−24
	52	3	59	43	44	52	3	60	44	45
τ (^{31}P)	−209	−249	−273	−249	−242	−195	−210	−254	−227	−222
	−194	−210	−255	−229	−223	−208	−248	−271	−248	−242
	403	459	528	477	465	403	458	525	475	464
τ (^{1}H(7))	−3	−4	−2	−1	−1	−3	−5	−3	−2	−2
	7	17	5	4	5	7	17	6	5	5
	−4	−13	−3	−3	−3	−4	−12	−3	−3	−3

This implies a broadening of the central pattern which is consistent with the absence of ^{13}C hyperfine splitting in the perpendicular region of the experimental spectrum and justifies the additional proton coupling used for the simulation of the frozen solution spectra.

These results unambiguously show that the neutral radical **4** obtained by capture of a proton by the primary negative ion is a much better candidate for the EPR spectra.

Conclusion

Although the EPR parameters measured with an electrochemically reduced solution of **1a** are not, *a priori*, inconsistent with the formation of the radical anion, the quantum-mechanics calculations clearly show that the hyperfine interactions for **3** are quite different from those calculated for $\mathbf{2}^-$ and that the experimental couplings are considerably more in accordance with the neutral allylic structure **4** than with that of the negatively charged species $\mathbf{2}^-$. In fact, this identification agrees

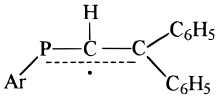

4

with two experimental results: (1) the cyclic voltammogram which reveals an irreversible reduction consistent with a rapid transformation of the anion. (2) The simulations of the frozen solution spectra which are consistent with an additional small coupling with a proton bound to the central carbon atom.

It is worthwhile commenting on the theoretical predictions for the two observables associated to the magnetic hyperfine interaction. Whereas single-determinant calculations may lead to acceptable values of the dipolar coupling tensors, we have seen here that the Fermi contact interaction varies considerably on passing from simple SCF, to Moller Plesset, and to CI calculations. Anisotropic coupling constants, which are better approximated by a single-determinant representation, are therefore considerably more pertinent than the Fermi contact for the identification of paramagnetic reaction intermediates at lower levels of theory. DFT calculations appear as an alternative to the more expensive CI treatments, especially for dipolar interactions.

Acknowledgment. We thank the Swiss National Science Foundation for financial support. The support of French CNRS-IDRIS is also greatly acknowledged.

References and Notes

(1) (a) *Multiple Bonds and Low Coordination in Phosphorus Chemistry*; Regitz, M., Scherer, O., Eds.; Thieme: New York, 1990. (b) Canac, Y.; Baceiredo, A.; Schoeller, W. W.; Gigmes, D.; Bertrand, G. *J. Am. Chem. Soc.* **1997**, *119*, 7579.

(2) (a) Nixon, J. F. *Chem. Rev.* **1988**, *88*, 1327. (b) Bourissou, D.; Canac, Y.; Collado, M. I.; Baceiredo, A.; Bertrand, G. *J. Am. Chem. Soc.* **1997**, *119*, 9923.

(3) (a) Geoffroy, M.; Jouaiti, A.; Terron, G.; Cattani-Lorente, M.; Ellinger, Y. *J. Phys. Chem.* **1992**, *96*, 8241. (b) Al Badri, A.; Chentit, M.; Geoffroy, M.; Jouaiti, A. *J. Chem. Soc., Faraday Trans.* **1997**, 93, 3631.

(4) Sidorenkova, H.; Chentit, M.; Jouaiti, A.; Terron, G.; Geoffroy, M.; Ellinger, Y. *J. Chem. Soc., Perkin 2* **1998**, 71.

(5) Appel, R.; Fölling, P.; Josten, B.; Siray, M.; Winkhaus, V.; Knoch, F. *Angew. Chem., Int. Ed. Engl.* **1984**, *23*, 619.

(6) Goede, S. J.; Bickelhaupt, F. *Chem. Ber.* **1991**, *124*, 2677.

(7) Yoshifuji, M.; Sasaki, S.; Inamoto, N. *Tetrahedron. Lett.* **1989**, *30*, 839.

(8) *WINEPR SimFonia* (version 1.25); Bruker Analytische Messtecknik Gmbh, 1996.

(9) Frisch, M. J.; Trucks, G. W.; Schlegel, H. B.; Gill, P. M. W.; Johnson, B. G.; Robb, M. A.; Cheeseman, J. R.; Keith, T.; Petersson, G. A.; Montgomery, J. A.; Raghavachari, K.; Al-Laham, M. A.; Zakrzewski, V. G.; Ortiz, J. V.; Foresman, J. B.; Ciolowski, J.; Stefanov, B. B.; Nanayakkara, A.; Challacombe, M.; Peng, C. Y.; Ayala, P. Y.; Chen, W.; Wong, M. W.; Andres, J. L.; Replogle, E. S.; Gomperts, R.; Martin, R. L.; Fox, D. J.; Binkley, J. S.; Defrees, D. J.; Baker, J.; Stewart, J. P.; Head-Gordon, M.; Gonzalez, C.; Pople, J. *Gaussian 94*, Revision B.1.; Gaussian Inc.: Pittsburgh, PA, 1995.

(10) Dupuis, M.; Johnston, F.; Marquez, A. *HONDO 8.5 from CHEM-Station*; IBM Corp.: Kingston, NY, 1994.

(11) McMurchie, L.; Elbert, S.; Langhoff, S.; Davidson, E. R. (modified by Feller, D.; Cave, R. J.; Rawlings, D.; Frey, R.; Daasch, R.; Nitzche, L.; Phillips, P.; Iberle, K.; Jackels, C.; Davidson, E. R.) *MELDF Suite of Programs;* 1990/91.

(12) Morton, J. R.; Preston, K. F. *J. Magn. Reson.* **1978**, *30*, 577.

(13) Chentit, M.; Sidorenkova, H.; Jouaiti, A.; Terron, G.; Geoffroy, M.; Ellinger, Y. *J. Chem. Soc., Perkin Trans. 2* **1997**, 921.

(14) Feller, D.; Huyser, E. S.; Borden, W. T.; Davidson, E. R. *J. Am. Chem. Soc.* **1983**, *105*, 1459.

(15) Nguyen, M. T.; Hegarty, A. F. *J. Chem. Soc., Perkin Trans. 2* **1985**, 1999.

(16) Bauschlicher, C. W.; Langhoff, S. R. *Spectrochim. Acta A* **1997**, 53, 1225.

(17) (a) Dunning, T. *J. Chem. Phys.* **1989**, *90*, 1007. (b) Kendall, R. A.; Dunning, T. H.; Harrison, R. J. *J. Chem. Phys.* **1992**, *96*, 6796.

(18) Parisel, O.; Giessner-Prettre, C.; Ellinger, Y. *Chem. Phys. Lett.* **1996**, *250*, 178.